On the Generalization of Common-Mode Rejection Analysis in CMOS Current Feedback Instrumentation Amplifiers

Apisak Worapishet

Mahanakorn Microelectronics Research Center (MMRC)
Mahanakorn University of Technology, Nongchok, Bangkok 10530, Thailand
E-mail: apisak@mut.ac.th

Manuscript received July 4, 2014
Revised August 5, 2014

ABSTRACT

A generalized analysis of the common-mode rejection performance due to both (trans-) conductance and capacitance mismatches in MOS transistor pairs is developed for the current-feedback instrumentation amplifiers (CFIAs). The generalized equations can be applied to the CFIAs with the current feedback path either via the drain terminals and the source terminals of the input stage. Such a generalization enables us to explore the optimum CFIA structure with a high CMRR for a specific application. Extensive verification of the developed equations is provided via practical simulation using BSIM MOS models, with excellent agreement between simulated and analytical results.

Keywords: *Instrumentation amplifiers*, *CMRR*, *CMRR analysis*, *CMOS amplifiers.*

1. INTRODUCTION

Instrumentation amplifiers (IA) are one of the indispensable building elements in bio-medical electronics. It serves as a front amplifier to amplify a typically very low-level bio-medical signal emanated from a sensor to a larger magnitude, in order to enable further processing, such as filtering and analog-to-digital conversion [1], [2]. Thus, the IA needs to possess a low noise performance. In addition, the IA must also have a capability to suppress large common-mode signals normally present along with the required signal.

Current-feedback IA (CFIA) uses both isolation and balancing technique as opposed to resistive-feedback IA which employs only balancing scheme. This makes the CFIA more superior in terms of the CMRR performance. Fig. 1(a) to 1(d) summarize the schematics of all the existing CFIA structures reported in the literature [3] – [7]. These are illustrated in CMOS implementations. Upon inspecting the IA structures, important observations can be made as follows. First, all the CFIA makes use of the resistive degenerated differential MOS pair as the differential input stage. Secondly, pMOS transistors are preferable due to their relatively low flicker noise as compared to the nMOS counterparts. Thirdly, the drain networks of the CFIAs are either a resistive load formed by diode-connected transistors [3], [4] and current source transistors [7], or an active load formed by current mirror transistors [6]. Finally, all the CFIAs rely upon a high-gain negative feedback loop to enable a high precision gain, where the feedback path can be either via the drain terminals [4] or the source terminals [3], [5] – [7].

From the above description, it may be deduced that all the CFIA structures share the same input differential pair, whereas their major differences lie in the feedback path, and the types of the drain/source networks. This, together with the fact that the common-mode rejection performance is primarily determined by mismatches (either systematic or random types) of the input stage, has opened up a possibility to derive a generalized CFIA structure that can enable us to derive a set of unified expressions for the CMRR performances of all the existing CFIAs. This should enable us to determine the optimum CFIA design with the minimum power requirement for a specific CMRR performance. More importantly, the unified analysis could allow us to explore the CFIA structures to search for the structure that provides both high CMRR and low power performances

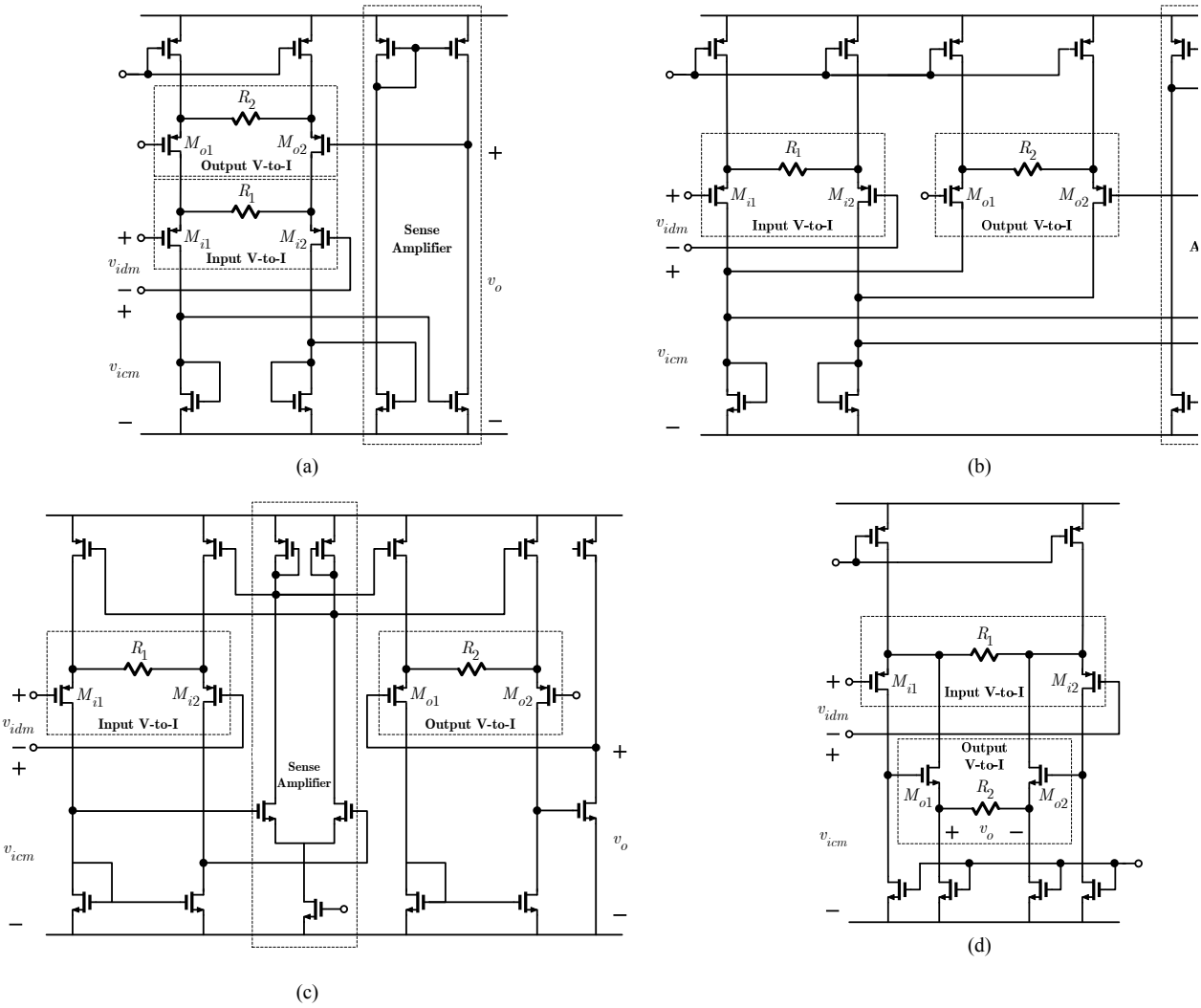

Fig. 1 *CMOS CFIA schematics of (a) direct CFIA [3], (b) indirect CFIA [4], (c) local feedback CFIA [5], [6], and (d) recent direct CFIA implementation [7].*

2. FORMULATION OF THE GENERALIZED CFIA EQUATIONS FOR COMMON-MODE RESPONSE ANALYSIS

2.1 *Description of the generalized current-feedback CFIA's input stage*

Fig. 2(a) shows the generalized input stage of the CFIA where it is essentially a resistively degenerated CMOS differential pair with the drain network as a load, and the source network as a current source (biasing). The voltages at the drain terminals are sensed by the amplifier A to the output. As indicated, the output feedback path can be via the source terminals i_{fs} (classified as the direct feedback configuration), or the drain terminals i_{fd}, (classified as the *in*direct feedback configuration), depending on the CFIA configurations under consideration.

Fig. 2(b) shows the small-signal analysis model for the generalized input stage of Fig. 2(a). It is noticed that, without affecting the analysis results, the drain and source networks are flipped, and this is for analysis convenience. Note that all the parasitic capacitances are included to enable a study of the high-frequency mismatch effects. C_{gs} and C_{gd} are the capacitances of the MOS transistors where C_s and C_d are the *total* capacitances of the source/drain terminals including those from the load/source or amplifier stages that are connected to the terminals. By applying KCL at each of the CFIA nodes, the basic equations are derived as summarized in (1) to (4) of the next page.

The expressions for $i_{d1,2}$ in (3) and (4) is dependent on the type of the load network. For a resistive load, i_{mr}

in Fig. 2(b) is set to zero. For a current-mirror load, we have $i_{mr} = v_{d1}/ r_{d1}$ and the conditions $r_{d2} >> r_{d1}$.

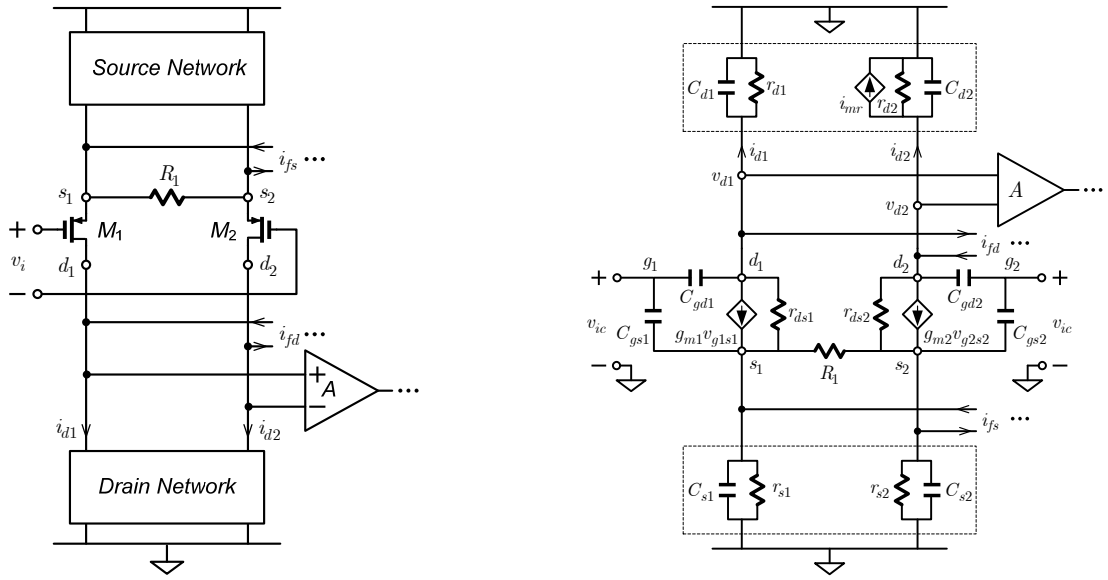

Fig. *2 Generalized CFIA input stage (a) schematic and (b) small-signal model*

KCL node s_1:
$$(g_{m1} + j\omega C_{gs1})(v_{ic} - v_{s1}) + \frac{(v_{d1} - v_{s1})}{r_{ds1}} - \left(\frac{1}{r_{s1}} + j\omega C_{s1}\right)v_{s1} - \frac{v_{s1} - v_{s2}}{R_1} + i_{fs} = 0 \quad (1)$$

KCL node s_2:
$$(g_{m2} + j\omega C_{gs2})(v_{ic} - v_{s2}) + \frac{(v_{d2} - v_{s2})}{r_{ds2}} - \left(\frac{1}{r_{s2}} + j\omega C_{s2}\right)v_{s2} - \frac{v_{s2} - v_{s1}}{R_1} - i_{fs} = 0 \quad (2)$$

KCL node d_1:
$$g_{m1}(v_{ic} - v_{s1}) - j\omega C_{gd1}(v_{ic} - v_{d1}) + \frac{(v_{d1} - v_{s1})}{r_{ds1}} + i_{d1} + i_{fd} = 0 \quad (3)$$

KCL node d_2:
$$g_{m2}(v_{ic} - v_{s2}) - j\omega C_{gd2}(v_{ic} - v_{d2}) + \frac{(v_{d2} - v_{s2})}{r_{ds2}} + i_{d2} - i_{fd} = 0 \quad (4)$$

To systematize the common-mode analysis, we have chosen to put mismatches into the equations via the following definitions:

$g_{m1} = g_m(1 - \sigma_{gm}/2)$, $g_{m2} = g_m(1 + \sigma_{gm}/2)$

$r_{ds1} = r_{ds}(1 - \sigma_{rds}/2)$, $r_{ds2} = r_{ds}(1 + \sigma_{rds}/2)$

$r_{s1} = r_s(1 + \sigma_{rs}/2)$, $r_{s2} = r_s(1 - \sigma_{rs}/2)$

$r_{d1} = r_d(1 - \sigma_{rd}/2)$, $r_{d2} = r_d(1 + \sigma_{rd}/2)$

$C_{gs1} = C_{gs}(1 + \sigma_{cgs}/2)$, $C_{gs2} = C_{gs}(1 - \sigma_{cgs}/2)$

$C_{gd1} = C_{gd}(1 + \sigma_{cgd}/2)$, $C_{gd2} = C_{gd}(1 - \sigma_{cgd}/2)$

$C_{s1} = C_s(1 - \sigma_{cs}/2)$, $C_{s2} = C_s(1 + \sigma_{cs}/2)$

$C_{d1} = C_d(1 + \sigma_{cd}/2)$, $C_{d2} = C_d(1 - \sigma_{cd}/2)$

where $\sigma_x = \Delta x / x$. Note that the mismatch signs defined above result in *cumulative* contributions of each mismatch.

By taking the sum and the difference between the KCL equations in (1) – (4) at the drain nodes and the source nodes, we have (5) to (8).

KCL node (s_1+s_2):

$$(g_{m1}v_{ic} + g_{m2}v_{ic}) - (g_{m1}v_{s1} + g_{m2}v_{s2}) + \left(\frac{v_{d1}}{r_{ds1}} + \frac{v_{d2}}{r_{ds2}}\right) - \left(\frac{v_{s1}}{r_{ds1}} + \frac{v_{s2}}{r_{ds2}}\right) - \left(\frac{v_{s1}}{r_{s1}} + \frac{v_{s2}}{r_{s2}}\right)$$
$$+j\omega(C_{gs1}v_{ic} + C_{gs2}v_{ic}) - j\omega(C_{gs1}v_{s1} + C_{gs2}v_{s2}) - j\omega(C_{s1}v_{s1} + C_{s2}v_{s2}) = 0 \quad (5)$$

KCL node (d_1+d_2):

$$(g_{m1}v_{ic} + g_{m2}v_{ic}) - (g_{m1}v_{s1} + g_{m2}v_{s2}) + \left(\frac{v_{d1}}{r_{ds1}} + \frac{v_{d2}}{r_{ds2}}\right) + (i_{d1} + i_{d2}) - \left(\frac{v_{s1}}{r_{ds1}} + \frac{v_{s2}}{r_{ds2}}\right)$$
$$-j\omega(C_{gd1}v_{ic} + C_{gd2}v_{ic}) + j\omega(C_{gd1}v_{d1} + C_{gd2}v_{d2}) = 0 \quad (6)$$

KCL node ($s_1 - s_2$):

$$(g_{m1}v_{ic} - g_{m2}v_{ic}) - (g_{m1}v_{s1} - g_{m2}v_{s2}) + \left(\frac{v_{d1}}{r_{ds1}} - \frac{v_{d2}}{r_{ds2}}\right) - \left(\frac{v_{s1}}{r_{ds1}} - \frac{v_{s2}}{r_{ds2}}\right) - \left(\frac{v_{s1}}{r_{s1}} - \frac{v_{s2}}{r_{s2}}\right)$$
$$+j\omega(C_{gs1}v_{ic} - C_{gs2}v_{ic}) - j\omega(C_{gs1}v_{s1} - C_{gs2}v_{s2}) - j\omega(C_{s1}v_{s1} - C_{s2}v_{s2}) = 0 \quad (7)$$
$$-2\left(\frac{v_{s1} - v_{s2}}{R_1}\right) + 2i_f = 0$$

KCL node ($d_1 - d_2$):

$$(g_{m1}v_{ic} - g_{m2}v_{ic}) - (g_{m1}v_{s1} - g_{m2}v_{s2}) + \left(\frac{v_{d1}}{r_{ds1}} - \frac{v_{d2}}{r_{ds2}}\right) + (i_{d1} - i_{d2}) - \left(\frac{v_{s1}}{r_{ds1}} - \frac{v_{s2}}{r_{ds2}}\right)$$
$$-j\omega(C_{gd1}v_{ic} - C_{gd2}v_{ic}) + j\omega(C_{gd1}v_{d1} - C_{gd2}v_{d2}) \quad (8).$$
$$+2i_{fd} = 0$$

Based on the mismatch definitions, we can approximate the sum and difference terms as summarized in the Appendix. By dividing the sum and the difference of the KCL equations by two, and applying the approximations into (5) – (8), we obtain (9) to (12).

KCL node (s_1+s_2)/2:
$$\left(g_m + \frac{1}{r_{ds}} + \frac{1}{r_s} + j\omega C_{gs} + j\omega C_s\right)v_s - \frac{1}{r_{ds}}v_d = (g_m + j\omega C_{gs})v_{ic} \quad (9)$$

KCL node (d_1+d_2)/2:
$$\left(g_m + \frac{1}{r_{ds}}\right)v_s - \left(\frac{1}{r_{ds}} + j\omega C_{gd}\right)v_d - i_d = (g_m - j\omega C_{gd})v_{ic} \tag{10}$$

KCL node (s_1–s_2)/2:
$$\begin{aligned}&\left(g_m + \frac{2}{R_1} + \frac{1}{r_{ds}} + \frac{1}{r_s} + j\omega C_{gs} + j\omega C_s\right)\frac{dv_s}{2} - \frac{1}{r_{ds}}\frac{dv_d}{2} - i_{fs}\\ &+ \underbrace{\frac{\sigma_{gm}}{2}g_m(v_{ic} - v_s)}_{i_{\sigma gm}} - \underbrace{\frac{\sigma_{rds}}{2r_{ds}}(v_d - v_s)}_{i_{\sigma rds}} - \underbrace{\frac{\sigma_{rs}}{2r_s}v_s}_{i_{\sigma rs}} - \underbrace{j\omega\frac{\sigma_{cgs}C_{gs}}{2}(v_{ic} - v_s)}_{i_{\sigma cgs}} - \underbrace{j\omega\frac{\sigma_{cs}C_s}{2}v_s}_{i_{\sigma cs}} = 0\end{aligned} \tag{11}$$

KCL node (d_1–d_2)/2:
$$\begin{aligned}&\left(g_m + \frac{1}{r_{ds}}\right)\frac{dv_s}{2} - \left(\frac{1}{r_{ds}} + j\omega C_{gd}\right)\frac{dv_d}{2} - \frac{di_d}{2} - i_{fd}\\ &+ \underbrace{\frac{\sigma_{gm}}{2}g_m(v_{ic} - v_s)}_{i_{\sigma gm}} - \underbrace{\frac{\sigma_{rds}}{2r_{ds}}(v_d - v_s)}_{i_{\sigma rds}} + \underbrace{j\omega\frac{\sigma_{cgd}C_{gd}}{2}(v_{ic} - v_d)}_{i_{\sigma cgd}} = 0\end{aligned} \tag{12}$$

, where $i_d = (i_{d1} + i_{d2})/2$ and $di_d = (i_{d1} - i_{d2})/2$. It is seen that the CFIA equations are now reduced into compact forms by taking their sums and differences. Nevertheless, it is noticed that auxiliary relations are now required to express the sum and the difference of the drain current terms, i_d and di_d. These are dependent on the type of the drain load network.

For the resistive load, we have $i_{d1,2} = (1/r_{d1,2} + j\omega C_{d1,2})\, v_{d1,2}$ since $i_{mr} = 0$ [cf. Fig. 2(b)]. Thus, we obtain the sum term as

$$\begin{aligned}i_d &= \frac{\left(i_{d1} + i_{d2}\right)}{2}\\ &= \frac{1}{2}\left(\left(1 / r_{d1} + j\omega C_{d1}\right)v_{d1} + \left(1 / r_{d2} + j\omega C_{d2}\right)v_{d2}\right)\\ &\approx v_d / r_d + j\omega C_d v_d\end{aligned}$$

, and the difference term as

$$\begin{aligned}\frac{di_d}{2} &= \frac{\left(i_{d1} - i_{d2}\right)}{2}\\ &= \frac{1}{2}\left(\left(1 / r_{d1} + j\omega C_{d1}\right)v_{d1} - \left(1 / r_{d2} + j\omega C_{d2}\right)v_{d2}\right)\\ &\approx \frac{dv_d}{2r_d} + \underbrace{\sigma_{rd}\frac{v_d}{2r_d}}_{i_{\sigma rd}} + j\omega C_d\frac{dv_d}{2} + \underbrace{j\omega\frac{\sigma_{cd}C_d}{2}v_d}_{i_{\sigma cd}}\end{aligned}$$

Applying the above relations to (10) and (12), after rearrangement, we have a set of the general CFIA equations under the resistive load as shown in (13) to (16).

Common-mode equations:
$$\left(g_m + \frac{1}{r_{ds}} + \frac{1}{r_s} + j\omega C_{gs} + j\omega C_s\right)v_s - \frac{1}{r_{ds}}v_d = (g_m + j\omega C_{gs})v_{ic} \tag{13}$$

$$\left(g_m + \frac{1}{r_{ds}}\right)v_s - \left(\frac{1}{r_{ds}} + \frac{1}{r_d} + j\omega C_{gd} + j\omega C_d\right)v_d = (g_m - j\omega C_{gd})v_{ic} \tag{14}$$

Differential-mode equations:

$$\left(g_m + \frac{2}{R_1} + \frac{1}{r_{ds}} + \frac{1}{r_s} + j\omega C_{gs} + j\omega C_s\right)\frac{dv_s}{2} - \frac{1}{r_{ds}}\frac{dv_d}{2} - i_{fs} = -i_{\sigma gm} + i_{\sigma rds} + i_{\sigma rs} + i_{\sigma cgs} + i_{\sigma cs} \tag{15}$$

$$\left(g_m + \frac{1}{r_{ds}}\right)\frac{dv_s}{2} - \left(\frac{1}{r_{ds}} + \frac{1}{r_d} + j\omega C_{gd} + j\omega C_d\right)\frac{dv_d}{2} - i_{fd} = -i_{\sigma gm} + i_{\sigma rds} + i_{\sigma rd} - i_{\sigma cgd} + i_{\sigma cd} \tag{16}$$

Let us now consider the current-mirror load. We have $i_{d2} = (1-\sigma_{cm})v_{d1}/r_{d1} + v_{d2}/r_{d2} + j\omega C_{d2}v_{d2}$. Note that σ_{cm} is the mismatch in the current mirror transfer. Since it is typical that $r_{d2} >> r_{d1}$, we have $i_{d2} \approx (1-\sigma_{cm})v_{d1}/r_{d1} + j\omega C_{d2}v_{d2}$. So, we obtain

$$i_d = (i_{d1} + i_{d2})/2 \approx \frac{1}{2}\Big[\left(v_{d1}/r_{d1} + j\omega C_{d1}v_{d1}\right) + \left((1-\sigma_{cm})v_{d1}/r_{d1} + j\omega C_{d2}v_{d2}\right)\Big] \approx v_{d1}/r_d + j\omega C_d v_d \tag{17}$$

where $r_{d1} = r_d$ is set arbitrarily for convenience, and

$$\frac{di_d}{2} = \frac{(i_{d1} - i_{d2})}{2} = j\omega C_d\frac{dv_d}{2} + \underbrace{\frac{\sigma_{cm}}{2r_d}v_{d1}}_{i_{\sigma cm}} + \underbrace{j\omega\frac{\sigma_{cd}C_d}{2}v_d}_{i_{\sigma cd}} \tag{18}$$

After rearrangement, we now have the general equations for the common-mode CFIA analysis as shown in (19) to (22).

Common-mode equations:

$$\left(g_m + \frac{1}{r_{ds}} + \frac{1}{r_s} + j\omega C_{gs} + j\omega C_s\right)v_s - \frac{1}{r_{ds}}v_d = (g_m + j\omega C_{gs})v_{ic} \tag{19}$$

$$\left(g_m + \frac{1}{r_{ds}}\right)v_s - \left(\frac{1}{r_{ds}} + j\omega C_{gd} + j\omega C_d\right)v_d - \frac{v_{d1}}{r_d} = (g_m - j\omega C_{gd})v_{ic} \tag{20}$$

Differential-mode equations:

$$\left(g_m + \frac{2}{R_1} + \frac{1}{r_{ds}} + \frac{1}{r_s} + j\omega C_{gs} + j\omega C_s\right)\frac{dv_s}{2} - \frac{1}{r_{ds}}\frac{dv_d}{2} - i_{fs} = -i_{\sigma gm} + i_{\sigma rds} + i_{\sigma rs} + i_{\sigma cgs} + i_{\sigma cs} \tag{21}$$

$$\left(g_m + \frac{1}{r_{ds}}\right)\frac{dv_s}{2} - \left(\frac{1}{r_{ds}} + j\omega C_{gd} + j\omega C_d\right)\frac{dv_d}{2} - i_{fd} = -i_{\sigma gm} + i_{\sigma rds} - i_{\sigma cgd} + i_{\sigma cd}\,. \tag{22}$$

Table 1 *Unified common-mode feedback current responses for CFIAs*

Parameters	$i_{fs,fd}$ Expressions
g_m	$\eta\sigma_{gm}\cdot\dfrac{r_d+r_s+r_{ds}}{R_1\left(r_d+r_s+r_{ds}+g_m r_s r_{ds}\right)}$
r_{ds}	$\eta\sigma_{rds}\cdot\dfrac{r_d+r_s}{R_1\left(r_d+r_s+r_{ds}+g_m r_s r_{ds}\right)}$
r_s	$\eta\sigma_{rs}\cdot\dfrac{g_m r_{ds}}{2\left(r_d+r_s+r_{ds}+g_m r_s r_{ds}\right)}$
r_d	$\eta\sigma_{rd}\left(1+\dfrac{2}{g_m R_1}\right)\cdot\dfrac{g_m r_{ds}}{2\left(r_d+r_s+r_{ds}+g_m r_s r_{ds}\right)}$
C_{gs}	$\eta\pi f\sigma_{cgs}C_{gs}\cdot\dfrac{r_d+r_s+r_{ds}}{\left(r_d+r_s+r_{ds}+g_m r_s r_{ds}\right)}$
C_{gd}	$\eta\pi f C_{gd}\sigma_{cgd}\left(1+\dfrac{2}{g_m R_1}\right)\cdot\left(1+\dfrac{g_m r_d r_{ds}}{\left(r_d+r_s+r_{ds}+g_m r_s r_{ds}\right)}\right)$
C_s	$\eta\pi f\sigma_{cs}C_s\cdot\dfrac{g_m r_s r_{ds}}{\left(r_d+r_s+r_{ds}+g_m r_s r_{ds}\right)}$
C_d	$\eta\pi f C_d\sigma_{cd}\left(1+\dfrac{2}{g_m R_1}\right)\cdot\dfrac{g_m r_d r_{ds}}{\left(r_d+r_s+r_{ds}+g_m r_s r_{ds}\right)}$

The common-mode responses are also dependent upon the sensing condition of the amplifier *A* in Fig. 2(a) and 2(b). For a balanced sensing scheme, the amplifier *A* is of differential type and its input (+/–) terminals senses the voltage difference between the drain terminals. Typically, the differential gain of the amplifier is very high within the operating bandwidth of the CFIA, whereas the common-mode gain is very low (less than one). Following this, we have $v_{d1}\approx v_{d2}=v_d$, and thus, $dv_d=v_{d1}-v_{d2}\approx 0$, i.e., differential-mode virtual earth. For the recent direct CFIA with the differential output in [7], the gain of the amplifier *A* in the model of Fig. 2(a) is equivalent to unity. To obtain a high loop gain, the CFIA makes use of a large drain resistance r_d instead, and the differential drain voltage, dv_d, of the input stage is applied directly to the output stage to produce the feedback current. Following this, we have a finite value of dv_d as given by

$$i_{fs,d}=\frac{dv_s}{R_1}=\frac{1}{R_1}\cdot\frac{R_1}{(R_1+2/g_m)}dv_d=\gamma dv_d \tag{23}$$

It should be noted that an *un*balanced or single-ended sensing at the drain terminal of the input stage is also possible. However, as it will lead to systematic common-mode responses, this scheme is not feasible and hence is not of practical and analysis interest.

Table 2 *Approximated unified common-mode feedback current responses for CFIAs*

Parameters	$i_{fs,fd}$ Expressions
g_m	$\eta\sigma_{gm} \cdot \dfrac{1}{R_1 g_m (r_s \,\|\|\, r_{ds})}$
r_{ds}	$\eta\sigma_{rds} \cdot \dfrac{1}{R_1 g_m r_{ds}}$
r_s	$\eta\sigma_{rs} \cdot \dfrac{1}{2r_s}$
r_d	$\eta\sigma_{rd} \cdot \dfrac{1}{2r_s}\left(1+\dfrac{2}{g_m R_1}\right)$
C_{gs}	$\eta\pi f\sigma_{cgs} C_{gs} \cdot \dfrac{1}{g_m (r_s \,\|\|\, r_{ds})}$
C_{gd}	$\eta\pi f\sigma_{cgd} C_{gd} \cdot \left(1+\dfrac{2}{g_m R_1}\right)$
C_s	$\eta\pi f\sigma_{cs} C_s$
C_d	$\eta\pi f\sigma_{cd} C_d \cdot \dfrac{r_d}{r_s}\left(1+\dfrac{2}{g_m R_1}\right)$

3. ANALYSIS RESULTS OF THE GENERALIZED CFIA EQUATIONS

Based upon (13) to (22), the unified expressions for the current i_{fs} or i_{fd} under the common-mode input for each of the component mismatches can be derived as summarized in Table I. They can be applied for all the structures including the direct and local (*source* feedback) CFIA in [3], [6] and [7], the indirect (*drain* feedback) CFIA in [4], with both the resistive and current mirror loads. The structural dependent factor η is defined as follows. For the source feedback CFIAs, we have $\eta = 1$. For the drain feedback CFIA, we have

$$\eta = \frac{1}{\left(1 + 2 / g_m R_1\right)} \tag{24}$$

In fact, (24) reflects the current relation between the source and drain feedback currents, i_{fs} and i_{fd}. That is, with the use of the current division, the following relation can be shown for the circuit in Fig. 2(b):

$$i_{fd} = i_{fs} \frac{(R_1 / 2)}{\left(1 / g_m + R_1 / 2\right)} = \underbrace{\frac{1}{\left(1 + 2 / g_m R_1\right)}}_{\eta} i_{fs} \tag{25}$$

For the sake of completeness, it should be noted that for the source feedback direct CFIA in [7], as a result of the amplifier gain at unity, it can be shown that

$$\eta = \frac{1}{\left(1 + \left(\dfrac{1}{2} + \dfrac{1}{g_m R_1}\right)\left(\dfrac{1}{r_d} + \dfrac{1}{g_m R_1 (r_d \,\|\, r_{ds})}\right)\right)}. \tag{26}$$

To ease a comparison between each component mismatch, it is instructive to reduce the expressions by the condition that $r_d << r_s, r_{ds}$ which is of typical design condition in most practical IAs, except for the

structure in [7]. The approximated expressions are summarized in Table 2. In inspecting the table, one can deduce that, given the same percentage of component mismatch, those parameters associated with the input differential pair, particularly g_m, r_{ds} and C_{gd} are more dominant than the others.

Table 3 *Simulated versus calculated mismatch parameters for SCFIA with* $\Delta W / W = 0.02$, $\Delta V_t = 1\ \mathrm{mV}$ *for all transistor pairs.*

Mismatch parameters	Nominal values	Mismatch factors σ	
		Simulated	Calculated
I_d, I_{ds}	37.72 μA	+ 0.0212	+ 0.0216
I_s	37.72 μA	− 0.1005	− 0.0993
g_m	543.7 μS	+ 0.0204	+ 0.0208
r_{ds}	1.833 MΩ	− 0.0249	− 0.0216
r_d	6.873 kΩ	− 0.0193	− 0.0191
r_s	1.065 MΩ	+ 0.1069	+ 0.0993

Table 4 *Common-mode feedback currents of SCFIA based on simulated mismatch errors in Table 3*

Mismatch factors	Common-mode feedback current i_{fs} (SCFIA)		
	Simulation (Small-signal equivalent circuit)	Analytical Calculation (Table II)	Simulation (Transistor level - BSIM3v3)
σ_{gm} (+ 0.0204)	− 139.1nA	− 138.9nA	**NA**
σ_{rds} (− 0.0249)	+ 62.65nA	+ 62.22nA	
σ_{rd} (− 0.0193)	+ 92.05nA	+ 91.95nA	
σ_{rs} (+ 0.1069)	+ 50.21nA	+ 50.19nA	
$\sum \sigma$	+ 65.85nA	+ 65.50nA	+ 62.65nA

4. ANALYSIS VERIFICATIONS

The compact form of the CMRR performance analysis equations developed in Section 3 is verified via simulation using BSIM3v3 MOS transistor models parameters from a standard 3.3-V 0.35-μm CMOS process. The simulated circuits for verification are based upon two practical configurations, i.e., the SCFIA in [6] (cf. Fig. 1(c)) and the DCFIA in [5] (cf. Fig. 1(b)), of which the schematics for simulations are shown in Fig. 4(a) and 4(b), respectively. To facilitate the investigation of each of the mismatch effect, deterministic mismatches. The analytical derivation is verified by incorporating systematic mismatch into the transistor pairs of the input V-to-I stages, by changing the widths and the threshold voltages where dc voltage sources are included at the gate terminals. As suggested with the help of simulation, transistor mismatches in the other stages have virtually no effect on the CMRR results.

Let us first begin with the (trans) conductance mismatches. Considering the SCFIA, the small-signal parameters for the input stage of the simulated SCFIA with nominal operation were extracted and these are given in Table 3. Also given in the table are the

simulated and calculated mismatches of the small-signal parameters using Table 2 with $\Delta W / W = 0.02$ and $\Delta V_t = 1\ \mathrm{mV}$ for all the transistor pairs in the input stage. Good agreement is observed with errors less than 14%. Table 4 shows the calculated feedback currents associated with each of the small-signal parameter mismatches in Table 3. As evident from Table 4, the overall calculated source feedback current is in close agreement with those obtained from simulation based on both the equivalent small-signal circuit and CMOS transistor schematic, thereby validating the integrity of the analysis.

Verification of the generalized CMRR analysis is also given through simulation of the DCFIA where the extracted small-signal parameters at nominal operation are given in Table 5. Similarly, with the same variation of the width and threshold voltage, it is evident that the simulated and calculated mismatches of the small-signal parameters are in close agreement with errors less than 4%. Also, as given in Table 4, the overall calculated and simulated drain feedback current of the DCFIA are in good agreement.

Table 5 *Simulated versus calculated mismatch parameters for DCFIA with* $\Delta W / W = 0.02$, $\Delta V_t = 1\ \mathrm{mV}$ *for all transistor pairs.*

Mismatch parameters	Nominal values	Mismatch factors σ	
		Simulated	Calculated
I_s	37.74 μA	+ 0.0331	+ 0.0346
I_{ds}	37.74 μA	+ 0.0342	+ 0.0368
I_d	37.74 μA	+ 0.0209	+ 0.0216
g_m	543.9 μS	+ 0.0294	+ 0.0284
r_{ds}	1.82 MΩ	− 0.0350	− 0.0368
r_d	3.498 kΩ	− 0.0189	− 0.0191
r_s	1.064 MΩ	− 0.0337	− 0.0346

Table 6 *Common-mode current responses based on simulated mismatch errors.*

Mismatch factors	Common-mode feedback current response i_{fs} (DCFIA)		
	Simulation Behavioral level	Calculation	Simulation Transistor level (BSIM3v3)
σ_{gm} (+ 0.0294)	− 19.71nA	− 19.74nA	**NA**
σ_{rds} (− 0.0350)	+ 8.68nA	+ 8.67nA	
σ_{rd} (− 0.0189)	+ 8.86nA	+ 8.88nA	
σ_{rs} (− 0.0337)	− 1.55nA	− 1.55nA	
$\sum \sigma$	− 3.73nA	− 3.74nA	− 3.95nA

Let us now turn to the capacitance mismatches. Table 7 shows the extracted nominal capacitances at the input stage of both the SCFIA and DCFIA. Note that to avoid the inherent capacitance mismatch associated with the drain current mirror load, a neutralization capacitor was added [8].

Table 7 *Extracted nominal capacitance values for SCFIA and DCFIA.*

Mismatch parameters	SCFIA	DCFIA
C_{gs}	2.43 pF	2.43 pF
C_{gd}	39.34 fF	39.34 fF
C_d	2.07 pF	2.07 pF
C_s	0.375 pF	0.375 pF

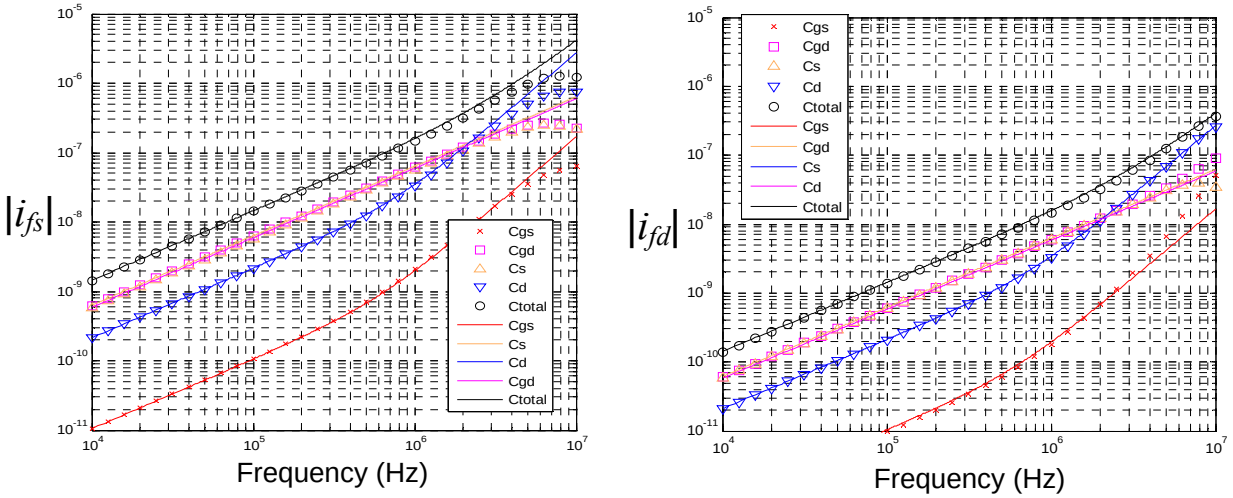

(a) (b)

Fig. 3 *(a) Simulated (legends) versus calculated (lines) high frequency common-mode current responses due to capacitance mismatches (all set at* $\Delta C / C = 0.05$*) for SCFIA, (b) simulated (legends) versus calculated (lines) high frequency common-mode current responses due to capacitance mismatches (all set at* $\Delta C / C = 0.05$*) for DCFIA.*

Fig. 3 (a) and 3 (b) show the simulated and calculated frequency responses of the source and drain common-mode feedback currents, respectively. For these plots, systematic capacitance mismatches at $\Delta C / C = 0.05$ were included in all the extracted capacitances in Table 7 by adding linear capacitors in parallel. It is evident from the simulated responses that the simulation and calculation based on Table II are in close agreement and thus the integrity of the analysis is verified.

5. CONCLUSIONS

A generalized analysis of the common-mode rejection ratio (CMRR) performance due to both (trans-) conductance and capacitance mismatches is developed for the current-feedback instrumentation amplifiers (CFIAs). The generalized equations can be applied to the CFIAs with the current feedback path either via the drain terminals and the source terminals of the input stage. Such a generalization enables us to explore the optimum CFIA structure with a high CMRR for a specific application. Extensive verification of the developed equations is provided via practical simulation using BSIM MOS models, with excellent agreement between simulated and analysis results.

6. APPENDIX

The derivations of the approximated sum and difference expressions employed in the analysis of this paper are given as follows:

1) $(g_{m1}v_1 + g_{m2}v_2)$

$$= \underbrace{\left(g_m \pm \sigma g_m / 2\right)v_1}_{g_{m1}v_1} + \underbrace{\left(g_m \mp \sigma g_m / 2\right)v_2}_{g_{m2}v_2}$$
$$= g_m v_1 \pm \sigma g_m v_1 / 2 + g_m v_2 \mp \sigma g_m v_2 / 2$$
$$= g_m \underbrace{(v_1 + v_2)}_{2v} \pm \sigma g_m \underbrace{(v_1 - v_2)}_{dv} / 2$$
$$= 2g_m v \pm \underbrace{\sigma g_m dv / 2}_{0} \approx 2g_m v$$

2) $\left(v_1 / r_1 + v_2 / r_2\right)$

$$= \left(\frac{v_1}{r \mp \sigma r / 2} + \frac{v_2}{r \pm \sigma r / 2}\right)$$
$$\approx \frac{v_1}{r}(1 \pm \sigma / 2) + \frac{v_2}{r}(1 \mp \sigma / 2)$$
$$= \frac{1}{r}\left(v_1 \pm \sigma v_1 / 2 + v_2 \mp \sigma v_2 / 2\right)$$
$$= \frac{1}{r}\left(\left(v_1 + v_2\right) \pm \sigma\left(v_1 - v_2\right) / 2\right)$$
$$= \frac{2v}{r} \pm \underbrace{\frac{\sigma dv / 2}{r}}_{0} \approx \frac{2v}{r}$$

3) $(C_1 v_1 + C_2 v_2)$

$$= \underbrace{\left(C \pm \sigma C / 2\right)v_1}_{C_1 v_1} + \underbrace{\left(C \mp \sigma C / 2\right)v_2}_{C_2 v_2}$$
$$= Cv_1 \pm \sigma C v_1 / 2 + Cv_2 \mp \sigma C v_2 / 2$$
$$= C\underbrace{(v_1 + v_2)}_{2v} \pm \sigma C \underbrace{(v_1 - v_2)}_{dv} / 2$$
$$= 2Cv \pm \underbrace{\sigma C dv / 2}_{0} \approx 2Cv$$

4) $(g_{m1}v_1 - g_{m2}v_2)$

$$= \underbrace{\left(g_m \pm \sigma g_m / 2\right)v_1}_{g_{m1}v_1} - \underbrace{\left(g_m \mp \sigma g_m / 2\right)v_2}_{g_{m2}v_2}$$
$$= g_m v_1 \pm \sigma g_m v_1 / 2 - g_m v_2 \pm \sigma g_m v_2 / 2$$
$$= g_m(v_1 - v_2) \pm \sigma g_m(v_1 + v_2) / 2$$
$$= g_m dv \pm \sigma g_m v$$

5) $\left(v_1 / r_1 - v_2 / r_2\right)$

$$= \left(\frac{v_1}{r \mp \sigma r / 2} - \frac{v_2}{r \pm \sigma r / 2}\right)$$
$$\approx \frac{v_1}{r}(1 \pm \sigma / 2) - \frac{v_2}{r}(1 \mp \sigma / 2)$$
$$= \frac{1}{r}\left(v_1 \pm \sigma v_1 / 2 - v_2 \pm \sigma v_2 / 2\right)$$
$$= \frac{1}{r}\left(\left(v_1 - v_2\right) \pm \sigma\left(v_1 + v_2\right) / 2\right)$$
$$= \frac{dv}{r} \pm \sigma \frac{v}{r}$$

6) $(C_1 v_1 + C_2 v_2)$

$$= \underbrace{\left(C \pm \sigma C / 2\right)v_1}_{C_1 v_1} - \underbrace{\left(C \mp \sigma C / 2\right)v_2}_{C_2 v_2}$$
$$= Cv_1 \pm \sigma C v_1 / 2 - Cv_2 \pm \sigma C v_2 / 2$$
$$= C(v_1 - v_2) \pm \sigma C(v_1 + v_2) / 2$$
$$= Cdv \pm \sigma Cv$$

REFERENCES

[1] P. Kompitthaya, J. Mahattanakul, "Realization of adaptable 8-bit μ-law signed analog-to-digital converter," *Engineering Transactions*, vol. 11, No. 1(24), 2008.

[2] J. Mahattanakul, "Active-RC filter synthesis by section substitution method," *Engineering Transactions*, vol. 13, No. 2(29), 2010.

[3] M. S. J. Steyaert, W. M. C. Sansen, and C. Zhongyuan, "A micropower low-noise monolithic instrumentation amplifier for medical purposes," *IEEE J. Solid-State Circuits*, vol. sc-22, no. 6, pp. 1163-1168, Dec. 1987.

[4] B. J. van den Dool and J. H. Huijsing, "Indirect current feedback instrumentation amplifier with a common-mode input range that includes the negative rail," *IEEE J. Solid-State Circuits*, vol. 28, no. 7, pp. 743-749, July 1993.

[5] A. P. Brokaw and M. P. Timko, "An improved monolithic instrumentation amplifier," *IEEE J. Solid-State Circuits*, vol. sc-10, no. 6, pp. 417-423, Dec. 1975

[6] R. Martins, S. Selberherr, and F. A. Vaz, "A CMOS IC for portable EEG acquisition systems," *IEEE Trans. Instrum. Meas.*, vol. 47, no. 5, pp. 1191-1196, Oct. 1998.

[7] R. F. Yazicioglu, P. Merken, R. Puers, and C. V. Hoof, "A 60 μW 60nV/$\sqrt{}$Hz readout front-end for portable biopotential acquisition systems," *IEEE J. Solid-State Circuits*, vol. 42, no. 5, pp. 1100-1110, May 2007.

[8] A. Worapishet, A. Demosthenous and X, Liu, "A CMOS Instrumentation Amplifier With 90-dB CMRR at 2-MHz Using Capacitive Neutralization: Analysis, Design Considerations and Implementation", *IEEE Transactions on Circuits and Systems – I*: Regular Paper**.** Vol. 58, No. 4, pp. 699-710, April 2011.

Apisak Worapishet received the B.Eng. degree (with first-class honors) from King Mongkut's Institute of Technology Ladkrabang, Bangkok, Thailand, in 1990, the M.Eng.Sc. degree from the University of New South Wales, Australia, in 1995, and the Ph.D. degree from Imperial College, London, U.K., in 2000, all in electrical engineering. Since 1990, he has been with Mahanakorn University of Technology, Bangkok, Thailand. He currently serves as the Director of Mahanakorn Microelectronics Research Center (MMRC), and a Professor in Electronic Engineering. His current research interest includes mixed-signal CMOS analog integrated circuits, Bio-medical circuits, wirelined and wireless RF CMOS circuits, microwave circuits.